BIOCHEMISTRY
including biophysical chemistry & molecular biology
Article

Biochemistry **2010,** *49,* 539–546 539
DOI: 10.1021/bi901503g

Structural Insights into Substrate Specificity and the *anti* β-Elimination Mechanism of Pectate Lyase[†,‡]

Arefeh Seyedarabi,[§] Teng Teng To,[§] Salyha Ali,[§,⊥] Syeed Hussain,[§,▽] Markus Fries,[§,#] Robert Madsen,[∥] Mads H. Clausen,[∥] Susana Teixteira,[⊥,@] Keith Brocklehurst,[§] and Richard W. Pickersgill*[,§]

[§]*School of Biological and Chemical Sciences, Queen Mary University of London, Mile End Road, London E1 4NS, United Kingdom,* [∥]*Department of Chemistry, Technical University of Denmark, DK-2800 Lyngby, Denmark,* [⊥]*Institut Laue Langevin, 6 rue Jules Horowitz, 38000 Grenoble, France, and* [@]*EPSAM, Keele University, Keele, Staffordshire ST5 5BG, United Kingdom* [▽]*Current address: AstraZeneca, Alderly Park, Cheshire SK10 4TF, United Kingdom.* [#]*Current address: Baxter BioScience, Biomedical Research Center, Uferstrasse 15, A-2304 Orth an der Donau, Austria.*

Received August 27, 2009; Revised Manuscript Received November 19, 2009

ABSTRACT: Pectate lyases harness *anti* β-elimination chemistry to cleave the α-1,4 linkage in the homogalacturonan region of plant cell wall pectin. We have studied the binding of five pectic oligosaccharides to *Bacillus subtilis* pectate lyase in crystals of the inactive enzyme in which the catalytic base is substituted with alanine (R279A). We discover that the three central subsites (−1, +1, and +2) have a profound preference for galacturonate but that the distal subsites can accommodate methylated galacturonate. It is reasonable to assume therefore that pectate lyase can cleave pectin with three consecutive galacturonate residues. The enzyme in the absence of substrate binds a single calcium ion, and we show that two additional calcium ions bind between enzyme and substrate carboxylates occupying the +1 subsite in the Michaelis complex. The substrate binds less intimately to the enzyme in a complex made with a catalytic base in place but in the absence of the calcium ions and an adjacent lysine. In this complex, the catalytic base is correctly positioned to abstract the C5 proton, but there are no calcium ions binding the carboxylate at the +1 subsite. It is clear, therefore, that the catalytic calcium ions and adjacent lysine promote catalysis by acidifying the α-proton, facilitating its abstraction by the base. There is also clear evidence that binding distorts the relaxed 2_1 or 3_1 helical conformation of the oligosaccharides in the region of the scissile bond.

Pectate lyases are carbon−oxygen lyases that harness *anti* β-elimination chemistry to cleave the α-1,4 glycosidic linkage between D-galacturonate (GalA) residues in the homogalacturonan region of the plant polysaccharide pectin (*1*). In the reaction scheme below, R and R′ are additional α-1,4-linked GalA residues.

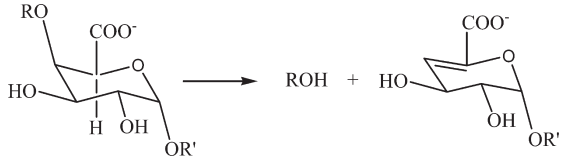

Pectate lyases play a pivotal role in remodeling and recycling the pectin polysaccharides present as insoluble composites in plant cell walls, accelerating rates of reaction by factors exceeding 10^{17}-fold and cleaving one of the most stable bonds in nature (*2*). The bacterial pectate lyases loosen the adhesion between plants cells, allowing the bacteria to invade causing crop spoilage. Pectate lyases (EC 4.2.2.2) occur in five of the 21 families of polysaccharide lyases (*3*): PL1, PL2, PL3, PL9, and PL10. *Bacillus subtilis* pectate lyase (BsPel),[1] the subject of this paper, belongs to PL1 and adopts the parallel β-helix fold (*4*, *5*); PL3 (*6*) and PL9 (*7*) pectate lyases also have this protein architecture as do fungal pectin lyases A and B (*8*, *9*), rhamnogalacturonase (GH28) (*10*), polygalacturonase (GH28) (*11*), and pectin methylesterase (CE8) (*12*−*15*). Pectate lyases in families PL2 and PL10 form $(\alpha,\alpha)_7$ and $(\alpha,\alpha)_3$ barrels, respectively (*16*, *17*).

The structure of pentagalacturonate in complex with *Erwinia chrysanthemi* pectate lyase C (PelC) has been reported previously (*18*), and a catalytic mechanism featuring abstraction of a proton from C5 of the GalA residue binding the +1 subsite with the elimination of the leaving group from C4 is reasonable (*19*). This reaction mechanism featuring proton abstraction by arginine acting as a base is supported by the convergence in active site geometry seen upon comparison of the PL10 and PL1 polysaccharide lyase structures (*17*). In this paper, we probe the mechanism and substrate specificity of BsPel in depth. We confirm the role of the catalytic base by observing its presence in the correct place for proton abstraction. We show that two

[†]This work was supported by a grant from the Biotechnological and Biology Sciences Research Council (Grant BBS/B/07896). The Higher Education Funding Council of England also supported this work.

[‡]Protein coordinates and structure factor amplitudes are available from the Protein Data Bank as entries 2NZM, 2O04, 2O0V, 2O17, 2O1D, and 3KRG.

*To whom correspondence should be addressed. Phone: ++44 20 7882 8444. Fax: +44 20 8983 0973. E-mail: r.w.pickersgill@qmul.ac.uk.

[1]Abbreviations: BsPel, *B. subtilis* pectate lyase; EDTA, ethylenediaminetetraacetic acid; Gal, galacturonate; GalMe, C6-methylated galacturonate; GalA3, trigalacturonate; GalA6, hexagalacturonate; HPLC, high-performance liquid chromatography; IPTG, isopropyl β-D-1-thiogalactopyranoside.

Published on Web 12/15/2009

Table 1: Crystallographic Data Statistics for the Six Oligosaccharide Soaks

	GalA3·3Ca	GalA6·3Ca	I·3Ca	II·3Ca	III·3Ca	GalA6·Co
resolution (Å)	2.0	2.3	1.8	1.7	1.9	1.9
R_{merge}[a,b] (%)	7.6 (13.8)	9.7 (22.0)	5.4 (11.7)	6.7 (24.1)	5.1 (14.6)	5.7 (6.7)
completeness[a] (%)	99.1 (97.6)	92.1 (90.3)	98.9 (98.4)	96.3 (83.4)	100.0 (100.0)	97.2 (96.1)
mean $I/\sigma(I)$[a]	15.7 (8.8)	11.0 (4.2)	19.7 (11.1)	15.0 (5.0)	18.4 (8.8)	23.8 (18.3)
R factor (R_{free})[c]	14.9 (19.7)	14.4 (22.3)	15.5 (18.5)	16.6 (20.1)	15.2 (19.2)	13.1 (19.6)

[a]Values in parentheses are for the highest-resolution shell. [b]$R_{merge} = (\sum_{hkl}\sum_i|I_i - \langle I\rangle|)/\sum_{hkl}\sum I_i$, where I_i is the intensity of the ith observation, $\langle I\rangle$ is the mean intensity of the reflection, and the summations extend over all unique reflections (hkl) and all equivalents (i). [c]R factor $= \sum_{hkl}|F_o - F_c|/\sum_{hkl}|F_o|$, where F_o and F_c represent the observed and calculated structure factors, respectively. The R factor is calculated using 95% of the data included in the refinement and R_{free} the 5% excluded. GalA3 and GalA6 are trigalacturonate and hexagalacturonate, respectively. The specifically methylated hexasacharrides (I, II, and III) are described in Materials and Methods. All complexes were formed in R279A crystals (catalytic base mutant) in the presence of calcium, with the exception of the last complex, GalA6·Co, formed in the triple mutant enzyme (N180A/D173A/K147A), in the absence of calcium (see the text for more details).

calcium ions that bind between the enzyme and substrate carboxylates at the +1 subsite together with an adjacent lysine residue stabilize the reaction intermediate. We also provide evidence that supports the view that substrate distortion is a characteristic of catalysis by pectate lyase. We show that the three central subsites (+2, +1, and −1) have a strong preference for galacturonate and that methylated galacturonate residues can be accommodated in the more distal subsites. Combining the results of crystallography, use of mutant enzymes, and isothermal titration calorimetry, we reveal the importance of entropy in binding and gain insight into the calcium binding characteristics of the free enzyme and the enzyme in the presence of substrate. The process of binding essential catalytic components, two calcium ions, together with substrate is uncommon in enzyme catalysis and is reminiscent of substrate-assisted catalysis.

MATERIALS AND METHODS

Production of Native and Mutant BsPel Proteins. A DNA fragment encoding the mature BsPel protein was amplified from *B. subtilis* genomic DNA using PCR and oligonucleotide primers that included NcoI restriction sites immediately flanking the coding sequence. The PCR product was subcloned into expression vector pET3d and the plasmid transformed into *Escherichia coli* BL21(DE3) pLysS. The sequence was confirmed before protein production. Protein overproduction was induced using IPTG (0.1 mM), and purification was conducted by ion exchange chromatography and size exclusion chromatography. Mutations were introduced using appropriate mutagenic primers and the QuickChange kit (Stratagene).

Kinetic Analyses. Enzyme assays using polygalacturonate were conducted at 42 °C in 50 mM Tris (pH 8.5) in the presence of 5 mM $CaCl_2$; the pH was checked for consistency before and after the assay. The formation of product was assessed at 235 nm (extinction coefficient of 5200 M^{-1} cm^{-1}). Acids were separated by HPLC using a calibrated Microsorb amino column. Unsaturated galacturonic acids were detected from their UV absorption at 232 nm.

Crystallography. Crystals of the R279A mutant were grown by streak seeding pre-equilibrated protein drops (20 mg/mL) using wild-type crystals as seeds. The soak conditions for the trigalacturonate complex were the reservoir conditions: 0.1 M sodium acetate (pH 4.6), 0.2 M ammonium acetate, and 18% PEG 4000, supplemented with 20 mM trigalacturonate, 7 mM calcium chloride, and 15% glycerol as a cryoprotectant. The conditions used for the hexasaccharide complexes were identical except that the hexasaccharide and calcium concentrations were 5 and 2 mM, respectively. The product complex used native crystals soaked under similar crystallization conditions supplemented with 20 mM GalA3, 5 mM sodium chloride, and 15% glycerol. The calcium-free complex was formed using the triple mutant which crystallized in the same space group and under soak conditions similar to those above with the exception that 2 mM cobalt chloride was used in place of calcium chloride, the hexagalacturonate concentration was increased to 100 mM, and the pH of the sodium acetate was lowered 0.6 unit to pH 4.0. The crystals, of space group $P2_1$ (a = 50.6 Å, b = 69.0 Å, c = 59.2 Å, and β = 113.6°) with one molecule in the asymmetric unit, were soaked in substrate for 10 min prior to being cryocooled and data collection.

Diffraction data were recorded at SRS Daresbury and ESRF Grenoble, and the crystallographic data are summarized in Table 1. Data were processed and reduced using MOSFLM (*20*) and SCALA (*21*), solved using MOLREP (*22*), and refined and visualized using REFMAC5/ARP (*23*, *24*) and O/COOT (*25*, *26*), respectively. In each case, calculated anomalous difference maps allowed the metal ions to be assigned unambiguously. Hexagalacturonate was produced as described previously (*27*). Three specifically methylated hexasaccharides (*28*−*31*) were also used: compound I, MMCCCM; compound II, CCMMMC; and compound III, MCCCCM (where M represents a methylated and C a nonmethylated galacturonate residue and the sequence is given starting from the nonreducing end of the hexasaccharide).

Isothermal Titration Calorimetry. Calcium ion binding to R279A BsPel and to R279A BsPel in the presence of 2 mM hexagalacturonate was assessed in 25 mM Tris-HCl (pH 7.5) and 100 mM NaCl at 25 °C using a MicroCal VP-ITC device. For the calcium titrations, the protein and hexasaccharide were dialyzed extensively against buffer supplemented with 1 mM EDTA and then against EDTA-free buffer before degassing and use. Heats of dilution were negligible for the titration of calcium into buffer and relatively small for the titration of calcium into hexasaccharide. The BsPel concentration used in these experiments was 0.13 mM.

RESULTS

Characterization of Mutant Proteins. We initially produced five mutants of BsPel to find an inactive but structurally unperturbed variant in which we could form enzyme−substrate complexes in the crystal (Table S1 of the Supporting Information). The residues chosen for mutation were the putative catalytic base, R279, and the three aspartates, 184, 223, and 227, that bind the single calcium seen in native BsPel. The R279A mutant had virtually no activity and only a minor perturbation of the active center, an increase in the mobility of Ile 250, and was

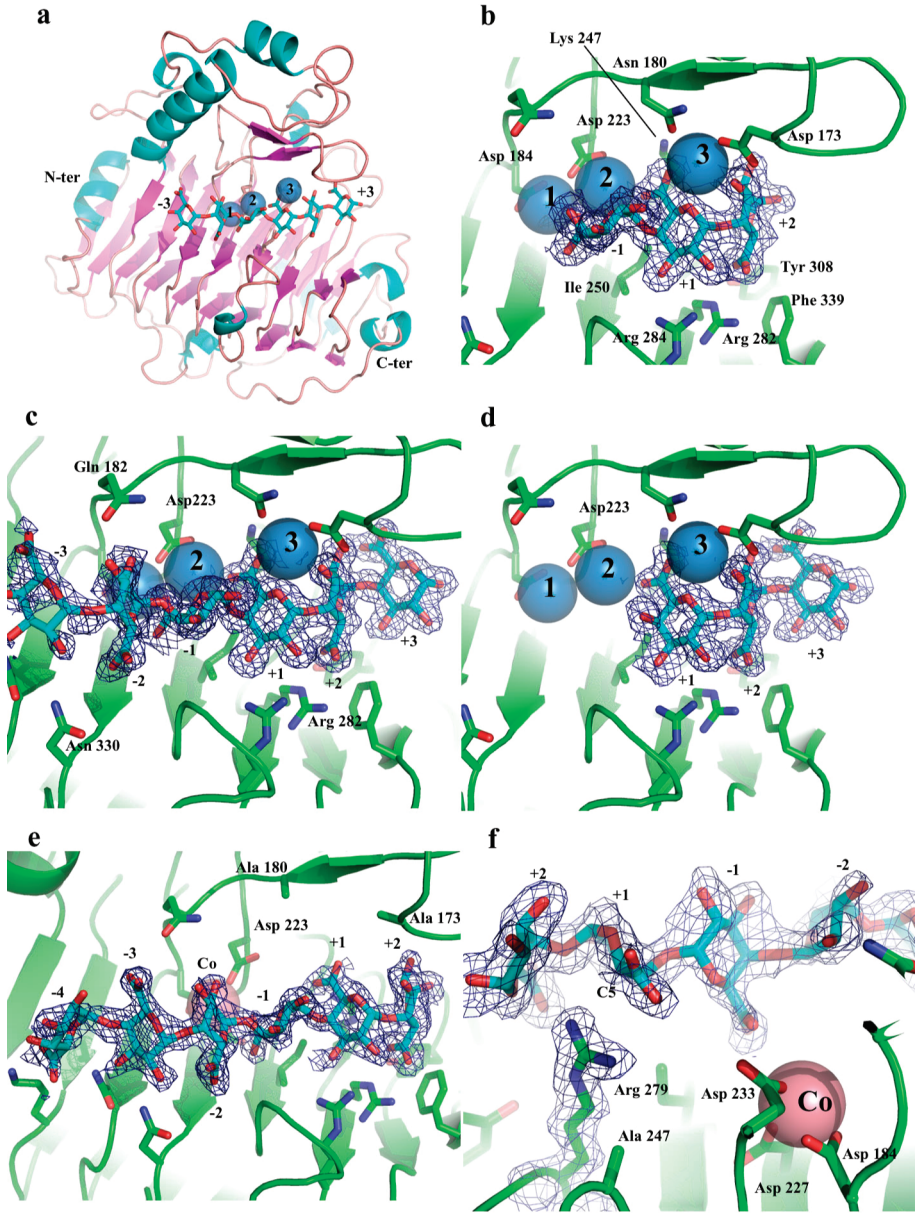

FIGURE 1: Pectin oligosaccharide binding to *B. subtilis* pectate lyase. Complexes shown in panels b–d were formed in crystals of the R279A (catalytic base mutant) form of BsPel. The complex shown in panels e and f was formed using the triple mutant (N180A/D173A/K247A) and cobalt in place of calcium. The maximum-likehood/σ_A-weighted $2F_o - F_c$ syntheses are contoured at 0.5σ for all apart from the GalA3 complex which is contoured at 1.0σ. All are shown as blue wire mesh. Calcium ions are shown as blue spheres, and cobalt is shown as the magenta sphere. (a) Cartoon representation of the parallel β-helix architecture of BsPel with β-strands and α-helices represented as magenta arrows and cyan helices, respectively. The cyan/red liquorice bonds represent bound hexasaccharide (pectin I). The oligosaccharide binds to the surface of the β-sheet known as PB1. The reducing end of the hexasaccharide binds toward the C-terminal end of the parallel β-helix. (b) GalA3, shown as cyan/red liquorice bonds, occupies subsites −1 to +2. Key side chains involved in binding are shown in stick representation. (c) Pectin I, a hexasaccharide with three consecutive carboxylates, binds to subsites −3 to +3. (d) Pectin II, hexasaccharide with only two consecutive carboxylates (see Materials and Methods), binds nonproductively to subsites +1 to +3. (e) GalA6 binding to the triple mutant (N180A/D173A/K277A) in the presence of cobalt (magenta sphere) which binds in place of calcium 1. The oligosaccharide binds to subsite +2 tightly but more loosely to subsites −4 to +1. The cobalt does not bind the −1 carboxylate directly, unlike calcium 1. (f) Enzyme's eye view of the complex shown in panel e. The experimental evidence for the location of the catalytic arginine and substrate is shown. Arginine 279 is ideally positioned to abstract the C5 proton from GalA binding in subsite +1. See the text for more details. This figure was produced using PyMOL (*47*).

therefore chosen for these studies. The R279K and D227A mutants had too much residual activity for preparation of complexes in the crystal. D223A had low activity and is a further candidate for preparation of the complexes in the crystal. Kinetic analysis of the wild-type enzyme showed that trigalacturonate was cleaved uniquely into unsaturated digalacturonate and saturated galacturonate, suggesting that trigalacturonate binds productively to subsites +2, +1, and −1. Digalacturonate was not cleaved at an appreciable rate and therefore presumably binds nonproductively or not at all. At pH 8.5 and in the presence of 5 mM Ca^{2+}, K_M and k_{cat} for trigalacturonate were 1.2 mM and 340 s^{-1}, respectively. K_M and k_{cat} for tetragalacturonate were 0.19 mM and 1000 s^{-1}, respectively; the k_{cat} value is similar to that measured using polygalacturonate (1200 s^{-1}). If the stability of pectin is on the order of 10 million years (*2*), then the rate enhancement is at least 10^{17}-fold.

Enzyme–Substrate Complexes Formed in the R279A Crystals. The inactive but structurally unperturbed mutant of

BsPel (R279A) was used to produce five enzyme−substrate complexes in the crystal (crystallographic details are given in Table 1). In each of these complexes, the substrates bind in the cleft formed by the surface of parallel β-sheet 1 and the adjacent loops, and two additional calcium ions are bound between the enzyme and oligogalacturonate (Figure 1a). Trigalacturonate binds to subsites −1, +1, and +2 (Figure 1b), in agreement with the measured kinetic data that showed that the product was an unsaturated digalacturonate and saturated galacturonate. Hexagalacturonate and pectins I and III bound subsites −3 to +3 (Figure 1c). Pectin II with only two consecutive GalA residues does not bind productively and occupied subsites +1 to +3 (Figure 1d). Continuous electron density was seen in maximum-likehood/σ_A-weighted $2F_o - F_c$ synthesis for GalA3. Five residues of the six were seen for GalA6 at 1.0σ with the sixth (subsite +3) weaker (mean *B* factors are given for each of the subsites in Table 2); five of six residues were seen for both pectins I and III at 1.0σ with weaker electron density for subsites away from the catalytic center. Maximum-likehood/σ_A-weighted $2F_o - F_c$ syntheses contoured at 1.0σ are shown for GalA3 and 0.5σ for pectin I and pectin II binding in Figure 1. The pectins superimpose on each other closely so that a description of the binding of subsites −1, +1, and +2 of pectin I is appropriate for all four productive complexes. The GalA carboxylate occupying the +1 subsite is bound by two calcium ions and K247 (Figures 1b and 2a). Both C2 and C3 hydroxyl groups form hydrogen bonds to R284 with the C2 hydroxyl close to the carboxyl binding subsite +2. At subsite +2, O3 binds the third calcium and the carboxylate oxygen atoms form hydrogen bonds to the NE and NH2 atoms of R282. At subsite −1 (leaving group), O5 binds the second calcium ion and the carboxylic O6A atoms bind to both the first and second calcium ions (Figures 1 and 2a and Table S2 of the Supporting Information).

Hexagalacturonate binds similarly to trigalacturonate, but in addition, subsites −2, −3, and +3 are occupied. Subsites −2 and −3 make fewer contacts with the enzyme than central sites +2, +1, and −1, and this is reflected in the mean *B* factors (Table 2). The partially methylated pectins I and III bind in a manner similar to that described for hexagalacturonate. Only subsites +3 to +1 are occupied for compound II, revealing that three consecutive carboxylates are needed for productive binding. No methyl groups were seen in the electron density for any of the specifically methylated compounds, probably due to rotation of

Table 2: Summary of the Binding of Pectic Oligosaccharides and Calcium to Pectate Lyase[a]

enzyme	substrate	−3	−2	−1	+1	+2	+3	metal
R279A	GalA3			C	C	C		3 Ca^{2+}
	B factor			9.7	8.8	9.3		
R279A	GalA6	C	C	C	C	C	C	3 Ca^{2+}
	B factor	41.3	28.2	13.1	12.4	13.9	30.0	
R279A	pectin I	M	M	C	C	C	M	3 Ca^{2+}
	B factor	47.9	37.5	17.2	10.9	9.4	22.3	
R279A	pectin II				C	C	M	3 Ca^{2+}
	B factor				28.6	25.5	34.7	
R279A	pectin III	M	C	C	C	C	M	3 Ca^{2+}
	B factor	46.1	34.9	17.7	10.4	8.9	24.9	
triple mutant	GalA6	C	C	C	C	C		1 Co^{2+}
	B factor	37.7	44.3	38.9	34.7	22.1		

[a]C and M indicate GalA and GalAMe, respectively. There is a strong preference for GalA at the +2, +1, and −1 subsites. Binding to the −3 subsite is seen only at low contour levels in the electron density maps. The *B* factors given here are the mean *B* factors of the atoms in the stated subsite in square angstroms. The isotropically refined *B* factor (*B*) is related to the mean square displacement of the atoms ($\langle u \rangle$) by the equation $B = 8\pi^2\langle u^2 \rangle$. The sixth GalA of GalA6 bound to the complex formed in the absence of calcium (Triple mutant) occupies the −4 subsite (see Figures 1e and 2b).

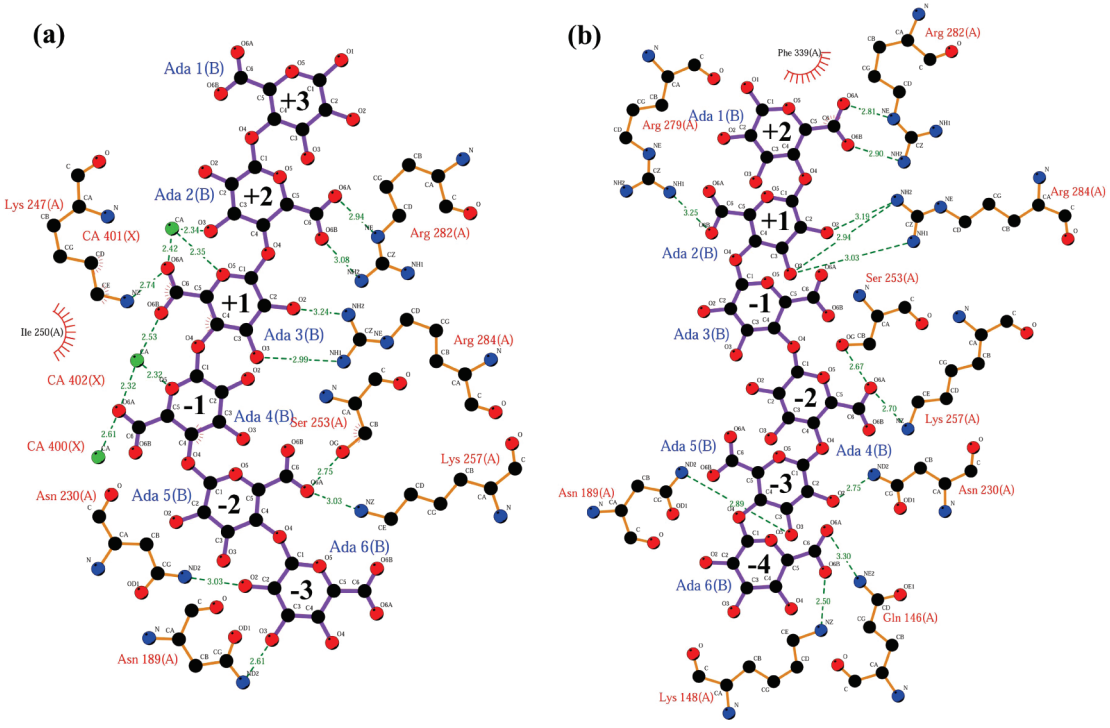

FIGURE 2: Schematic representation of the binding of hexaglacturonate to the R279A mutant and triple mutant in the absence of calcium (a and b, respectively). The molecular structures with corresponding density are shown in panels c and d of Figure 1, respectively. This figure was produced using LIGPLOT (*48*). Ligand bonds are colored blue and protein bonds brown; hydrogen bonds are drawn as dotted lines, and protein side chains involved in hydrophobic interactions are colored brown (for more information, see Figures S1−S4 of the Supporting Information).

Table 3: Torsion and Bond Angles about Selected Glycosidic Bonds[a]

oligosaccharide	subsites	ϕ (deg)	ψ (deg)	τ (deg)
GalA3	+1 to +2	115	153	124
	−1 to +1	63	58	130
pectin I	+1 to +2	118	151	118
	−1 to +1	75	45	140
pectin III	+1 to +2	119	150	120
	−1 to +1	70	52	137
PelC·GalA5	+1 to +2	117	157	117
PelC·GalA5	−1 to +1	73	51	120

[a]Torsion angles ϕ and ψ are about the C1−O4 and O4−C4 bonds, respectively. They are defined as O5′−C1′−O4−C4 (ϕ) and C1′−O4−C4−C5 (ψ), where the prime indicates atoms in the sugar residue toward the nonreducing end of the oligosaccharide. τ is the C1−O4−C4 bond angle. The ϕ and ψ angles of approximately 120° and 150°, respectively, correspond a 2_1 helical conformation of pectin (*18*, *44*−*46*). The ϕ and ψ angles of approximately 70° and 50°, respectively, correspond to a less-relaxed 6_1 helical conformation, if the angles are repeated. The values are shown for the complexes at 2.0 Å resolution, or better, and for the glycosidic bonds between the best-defined subsites −1, +1, and +2 as determined from analysis of *B* factors (Table 3). The values for PelC·GalA5 were taken from Table 1 of ref *18*, where the structure was refined at 2.2 Å resolution.

the methyl groups about the ester bond. The presence of the methyl groups is therefore inferred from the chemical structure of the specifically methylated hexasaccharides rather than by direct observation. LIGPLOT diagrams for the two GalA6 complexes appear in Figure 2 and for the other four complexes in the Supporting Information.

Calcium Binding Sites. Anomalous difference maps clearly revealed the presence of three calcium ions in the five enzyme−substrate complexes and a single calcium ion bound to the enzyme in absence of oligosaccharide. The first calcium binding site makes contacts with three aspartates (D184, D223, and D227), one water, and the carboxylate O6A atom of the GalA binding to subsite −1, although this is not a tight contact (Figure 1 and Table S2). D223 is the major contributor to the second calcium-binding site which binds tightly to the ring O5 and O6A atoms of the GalA in the −1 subsite and to the O6B atom of the GalA in the +1 subsite. The third calcium binds tightly to the O6A atom of the GalA in the +1 subsite and to the ring oxygen and carboxylate oxygen of the sugar residue in the +2 subsite. The stoichiometric enzyme:substrate:calcium ratio is 1:1:3 for these productive binding substrate complexes, and the structural and thermodynamic results together reveal that the three calcium ions have clearly defined roles in binding and catalysis. The mutational results suggest that changes to the environment of calcium 1 have significantly less impact on catalysis than those that affect calcium 2 (Table S1 and Figure 1) and that can be understood in terms of the number of tight contacts with calcium 2 in the enzyme−substrate complexes.

Conformation of the Pectic Oligosaccharides. The conformation of the pectic oligosaccharides bound in the substrate binding cleft adopts the expected relaxed 2_1 or 3_1 helical torsion angles with the important exception of those in the vicinity of the scissile bond (Table 3). If these torsion angles were repeated, the pectin helix would be approximately a 6_1 helix because when one looks down the chain the adjacent carboxylates in subsites −1 and +1 are rotated by approximately 60° with respect to one another rather than the 180° of the 2_1 helix or the 120° of the 3_1 helix. Evidence for distortion of the scissile bond comes first from a consideration of torsion angle ψ (C1′−O4−C4−C5, where prime indicates the GalA to the nonreducing side) which is within 45° of *cis* for the scissile bond as opposed to within 30° of *trans* for the other bonds and in the relaxed conformation of pectin (Table 3). Additionally, bond angle τ about the glycosidic oxygen (C1′−O−C4) is distorted from the anticipated value of 110−120° seen for the nonscissile bonds to 130−140° for the scissile bond (Table 3); this distortion is consistent with bringing the C1′ and C5 atoms close as a result of the 45° ψ angle. One must be careful in interpreting distortion observed in 1.8−2.0 Å ligand complex structures, but the conformation of the pectic oligosacharide is unusual and could result in distortion of the scissile bond.

Complex Formed in the Absence of the Calcium Ions. In an attempt to form a complex in the presence of the catalytic base (R279), the side chains forming the third calcium site (D173 and N180) were removed. The idea was that in the absence of one of the catalytic calcium ions the rate might be sufficiently low to enable the complex to be seen in the crystal with a catalytic base in place. The single mutants D173A and N180A and the double mutant D173A/N180N resulted in approximately 40, 30, and 5% of wild-type activity, respectively (Figure 1 and Table S1). K247 is also close to the substrate carboxylate bound by the third calcium. When the first two mutations were combined with a third mutation, K247A, to form the triple mutant, the activity dropped to 0.2% (Table S1). This residual activity still proved to be too great to produce complexes in the crystal. However, in the presence of 2 mM colbalt chloride in place of 1 mM calcium chloride, the complex could be trapped. This complex spans subsites −4 to +2 but is not as intimately bound to the active center as the other enzyme−substrate complexes (Figure 2), most obviously because the cobalt does not bind the −1 carboxylate and the two calcium ions bridging the substrate and enzyme carboxylates are absent (Figures 1 and 2). The conformation of the bound hexagalacturonate is closely similar to that seen in complexes in the presence of the two additional calcium ions, so the binding cleft is still distorting the pectin from the relaxed conformation in the region of the scissile bond despite the lack of oligosaccharide−calcium interactions. R279, clearly seen in the electron density map, is ideally positioned to abstract the C5 proton (Figure 1f).

Thermodynamic Measurements. Calcium binding to the first site of BsPel is stoichiometric and enthalpically driven with a K_d of 2.3 ± 0.1 μM (Figure S5 of the Supporting Information). Calcium binding to BsPel in the presence of a substrate gives a more complex binding curve, which cannot be fitted as a single process. As the crystal structure of the resulting complex is known (Figure 2a), the events can be interpreted in terms of the crystal structure. The binding can be modeled as a two-step process with first one calcium and then two additional calcium ions binding. This would correspond to the binding of calcium to site 1 first, followed by additional calcium ions binding to sites 2 and 3 as the enzyme−substrate complex is formed. Although the affinities are not accurately defined by the data, the first step is enthalpically driven and has an affinity comparable to that of the binding of calcium to the enzyme in the absence of substrate, and the second shows lower-affinity binding driven by entropic changes. (Figure S5). The thermodynamic parameters obtained from fitting the experimental data are listed in Table S3 of the Supporting Information.

DISCUSSION

Substitution of the catalytic arginine with alanine resulted in an enzyme with virtually no catalytic activity. Binding of pectic

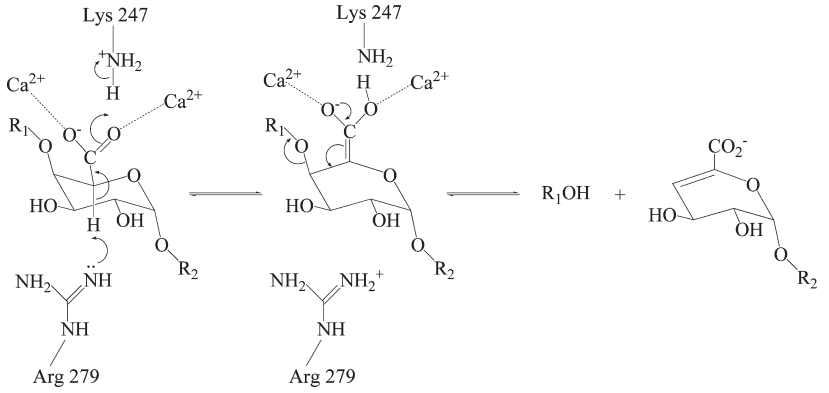

FIGURE 3: Plausible two-step mechanism for BsPel: (1) initial concerted abstraction of the α-proton and protonation of the carboxylic acid to generate an enol intermediate followed by (2) elimination of the β-leaving group from the enol. The intermediate is stabilized by the two catalytic calcium ions (calcium ions 2 and 3 which bind between the enzyme and substrate). One of these calcium ions may facilitate protonation of the leaving group.

oligosaccharides to crystals of the inactive enzyme showed that three consecutive substrate GalA residues are essential for productive binding to the calcium ions at subsites −1 and +1 and to the arginine at subsite +2. Outside these central subsites, methylated GalA residues can be accommodated. It is reasonable therefore to conclude that pectate lyase can cleave a pectin molecule with three of more consecutive GalA residues. The complex formed in crystals of the triple mutant protein lacking the calcium ions highlights the importance of the +2 subsite as the key substrate anchor. In fact, in every complex examined, the +2 subsite is occupied by GalA and the mean *B* factor for the +2 subsite is the lowest except for that of GalA3 where subsites −1 to +2 have similar values (Table 2). Pectin II binds to subsites +1, +2, and +3 yet still binds the catalytic calcium ions despite not binding to subsite −1. This binding mode is dictated by the preference of subsite +2 for GalA and the lack of three consecutive carboxylates in the oligosacharide. The importance of subsite +2 as the substrate anchor is further underlined by the observation that the same interaction between substrate carboxylate and arginine is seen in the family PL10 and PL3 complexes.

BsPel binds a single calcium ion, calcium 1, with an affinity (K_d) of 2.3 μM. This is substantially tighter than that measured indirectly for binding of the corresponding calcium to PelC (*32*). When calcium is titrated into the enzyme in the presence of substrate, two processes can be distinguished. The first is enthalpically driven with an affinity similar to that of the binding of the first calcium to BsPel; it is entirely plausible that this corresponds to the binding of the first calcium to BsPel. It is also plausible that the second process corresponds to the binding of the two additional calcium ions to form the Michealis complex. Remarkably, this second process is entropically driven, presumably due to the release of water from the surface of the hexasaccharide, calcium ions, and enzyme as the enzyme−substrate complex forms. Unlike most protein−carbohydrate interactions where there are aromatic residues involved in hydrophobic interactions, here there is an anionic substrate, a charged substrate binding cleft harboring a calcium ion, and two additional calcium ions that mediate the interactions between the enzyme and substrate. There is a single aliphatic hydrophobic residue, Ile 250, in the central part of the substrate-binding cleft of BsPel. Water molecules are released from the sugars binding the central subsites (+2, +1, and −1) and from the surface of the enzyme, and these are expected to contribute to the favorable entropic interaction. Water molecules are also released from the two calcium ions that are bound in the complex. The other binding sites are more waterlogged, and presumably favorable entropic changes are less significant here.

In the presence of calcium, the homogalacturonan region of pectin assumes a 2_1 helical conformation in dilute polymer solutions (*33*, *34*) and a 3_1 helix at higher concentrations in the gel or solid phase (*35*, *36*). More recent studies using nuclear magnetic resonance suggest the calcium−polygalacturonate complex in the plant cell wall contains both 2_1 and 3_1 helices as well as intermediate conformational states (*37*). Studies on di- and trisaccharides reveal similar helical conformations (*38*−*40*). There is clear evidence that the conformation of pectin is perturbed from relaxed 2_1 or 3_1 helical conformation by binding across the −1 and +1 subsites. The distortion from a helical 3_1 or 2_1 conformation is not simply a consequence of binding the second calcium because in the complex formed in the absence of calcium the conformation of the oligosaccharide is similar, showing the conformation is determined by the overall shape and characteristics of the binding cleft.

Catalysis by *B. subtilis* pectate lyase and by inference the family 1 polysaccharide lyases can be rationalized by a stepwise mechanism involving (i) initial concerted α-proton abstraction and protonation of the carboxylic acid to generate an enol intermediate followed by (ii) elimination of the β-leaving group from the enol (Figure 3). This is precisely as proposed by Gerlt and Gassman from consideration of the factors that would decrease the pK_a value of the α-proton and account for the observed rates of proton abstraction from a carbon adjacent to a carboxylate group (*41*, *42*). The crystallographic evidence for general base catalysis by R279 and general acid catalysis by R247 is strong, with both groups exquisitely poised for their respective functions (Figures 1 and 3).

The α-glycosidic linkage of the substrate and the C5 proton has ideal *anti* periplanar geometry for the *anti* β-elimination reaction catalyzed by pectate lyase to proceed. The conformation of the sugar in the +1 subsite must change from relaxed $^4C_1$ chair in the Michaelis complex to partially planar in the unsaturated product. A migration of C4 into the plane of C2, C3, and C5 would be the simplest change in conformation necessary for the reaction and would also be in accord with the principal of least nuclear motion during catalysis. Acidification of the α-proton by the catalytic calcium ions, especially the second calcium bound to both −1 and +1 carboxylates and D223, will lead to efficient transfer of a proton from C5 of the sugar in the +1 subsite to

R279. K247 appears to contribute to rate enhancement in the family 1 polysaccharide lyases by generating the more stable enol−enolate intermediate as opposed to the enolate−enolate intermediate, though it should be noted that the PL family 9 and 10 enzymes are active, albeit less so, with hydrogen bonding to the carboxylate from adjacent asparagines (*17*, *43*). A neutral lysine 247, neutral after protonation of the substrate carboxylate, proximal to the calcium ions, will also tend to stabilize the intermediate with respect to the Michaelis complex, thereby promoting catalysis.

The absence of an obvious group that protonates the glycosidic oxygen of the scissile bond is a concern because the alkoxide is a poor leaving group. The lone pair on the ring oxygen of the leaving group is *anti* periplanar to the C1−O4 bond, and the −1 GalA is intimately associated with calcium 2; these are both factors that will help to stabilize the leaving group. The closest group to either of the lone pairs of the glycosidic oxygen is the O3 hydroxyl from the sugar in the +1 subsite at a distance of 2.8 Å. The O3 hydroxyl might shuffle a proton from R284 and protonate the leaving group in a substrate-assisted protonation step that may be conserved between the family 1 and 10 lyases (*17*). However, given the intimate association of calcium and the GalA residue in the −1 subsite, protonation of the leaving group by solvent facilitated by calcium is also plausible.

ACKNOWLEDGMENT

We acknowledge the help given by Kathryn Worboys, Drummond Smith, Nicola Cummings, Ian Connerton, and John Jenkins in the early stages of this research and thank Alistair MacDougall for preparing the hexasaccharide used for the ITC studies. We acknowledge use of the ESRF Grenoble and SRS Daresbury for X-ray data collection.

SUPPORTING INFORMATION AVAILABLE

Additional results and analyses, Tables S1−S3, and Figures S1−S5. This material is available free of charge via the Internet at http://pubs.acs.org.

REFERENCES

1. Collmer, A., and Keen, N. T. (1986) The Role of Pectic Enzymes in Plant Pathogenesis. *Annu. Rev. Phytopathol. 24*, 383–409.
2. Wolfenden, R., and Snider, M. J. (2001) The depth of chemical time and the power of enzymes as catalysts. *Acc. Chem. Res. 34*, 938–945.
3. Cantarel, B. L., Coutinho, P. M., Rancurel, C., Bernard, T., Lombard, V., and Henrissat, B. (2009) The Carbohydrate-Active EnZymes database (CAZy): An expert resource for Glycogenomics. *Nucleic Acids Res. 37*, D233–D238.
4. Yoder, M. D., Keen, N. T., and Jurank, F. (1993) New domain motif: The structure of pectate lyase C, a secreted plant virulence factor. *Science 260*, 1503–1507.
5. Pickersgill, R. W., Jenkins, J., Harris, G., Nasser, W., and Robert-Baudouy, J. (1994) The structure of *Bacillus subtilis* pectate lyase in complex with calcium. *Nat. Struct. Biol. 1*, 717–723.
6. Akita, M., Suzuki, A., Kobayashi, T., Ito, S., and Yamane, T. (2001) The first structure of pectate lyase belonging to polysaccharide lyase family 3. *Acta Crystallogr. D57*, 1786–1792.
7. Jenkins, J., Shevchik, V. E., Hugouvieux-Cotte-Pattat, N., and Pickersgill, R. W. (2004) The crystal structure of pectate lyase Pel9A from *Erwinia chrysanthemi*. *J. Biol. Chem. 279*, 9139–9145.
8. Mayans, O., Scott, M., Connerton, I., Gravesen, T., Benen, J., Visser, J., Pickersgill, R., and Jenkins, J. (1997) Two crystal structures of pectin lyase A from *Aspergillus* reveal a pH driven conformational change and striking divergence in the substrate-binding clefts of pectin and pectate lyases. *Structure 5*, 677–689.
9. Vitali, J., Schick, B., Kester, H. C. M., Visser, J., and Jurnak, F. (1998) The three-dimensional structure of *Aspergillus niger* pectin lyase B at 1.7-angstrom resolution. *Plant Physiol. 116*, 69–80.
10. Petersen, T. N., Kauppinen, S., and Larsen, S. (1997) The crystal structure of rhamnogalacturonase A from *Aspergillus aculeatus*: A right-handed parallel β helix. *Structure 5*, 533–544.
11. Pickersgill, R., Smith, D., Worboys, K., and Jenkins, J. (1998) Crystal structure of polygalacturonase from *Erwinia carotovora ssp. carotovora*. *J. Biol. Chem. 273*, 24660–24664.
12. Jenkins, J., Mayans, O., Smith, D., Worboys, K., and Pickersgill, R. W. (2001) Three-dimensional structure of *Erwinia chrysanthemi* pectin methylesterase reveals a novel esterase active site. *J. Mol. Biol. 305*, 951–960.
13. Johansson, K., El-Ahmad, M., Friemann, R., Jornvall, H., Markovic, O., and Eklund, H. (2002) Crystal structure of plant pectin methylesterase. *FEBS Lett. 514*, 243–249.
14. Fries, M., Ihrig, J., Brocklehurst, K., Shevchik, V. E., and Pickersgill, R. W. (2007) Molecular basis of the activity of the phytopathogen pectin methylesterase. *EMBO J. 26*, 3879–3887.
15. Jenkins, J., and Pickersgill, R. (2001) The architecture of parallel β-helices and related folds. *Prog. Biophys. Mol. Biol. 77*, 111–175.
16. Abbott, D. W., and Boraston, A. B. (2007) A family 2 pectate lyase displays a rare fold and transition metal-assisted β-elimination. *J. Biol. Chem. 282*, 35328–35336.
17. Charnock, S. J., Brown, I. E., Turkenburg, J. P., Black, G. W., and Davies, G. J. (2001) Characterization of a novel pectate lyase, Pel10A, from *Pseudomonas cellulosa*. *Proc. Natl. Acad. Sci. U.S.A. 99*, 12067–12072.
18. Scavetta, R. D., Herron, S. R., Hotchkiss, A. T., Kita, N., Keen, N. T., Benen, J. A., Kester, H. C., Visser, J., and Jurank, F. (1999) Structure of a plant cell wall fragment complexed to pectate lyase C. *Plant Cell 11*, 1081–1092.
19. Herron, S., Benen, J. A., Scavetta, R. D., Visser, J., and Jurank, F. (2000) Structure and function of pectic enzymes: Virulence factors of plant pathogens. *Proc. Natl. Acad. Sci. U.S.A. 97*, 8762–8769.
20. Leslie, A. G. (1999) Integration of macromolecular diffraction data. *Acta Crystallogr. D55*, 240–255.
21. Evans, P. (2006) Scaling and assessment of data quality. *Acta Crystallogr. D62*, 72–82.
22. Vagin, A. A., and Teplyakov, A. (1997) MOLREP: An automated program for molecular replacement. *J. Appl. Crystallogr. 30*, 1022–1025.
23. Murshudov, G. N., Vagin, A. A., and Dodson, E. J. (1997) Refinement of macromolecular structures by the maximum-likelihood method. *Acta Crystallogr. D53*, 240–255.
24. Perrakis, A., Morris, R., and Lamzin, V. S. (1999) Automated protein model building combined with iterative structure refinement. *Nat. Struct. Biol. 6*, 458–463.
25. Jones, T. A., Zou, J.-Y., and Kjeldgaard, M. (1991) Improved methods for building protein models in electron density maps and the location of errors in these models. *Acta Crystallogr. A47*, 110–119.
26. Emsley, P., and Cowtan, K. (2004) Coot: Model-building tools for molecular graphics. *Acta Crystallogr. D60*, 2126–2132.
27. Rigby, N. M., MacDougall, A. J., Ring, S. G., Cairns, P., Morris, R., and Gunning, P. A. (2000) Observations on the crystallization of oligogalacturonates. *Carbohydr. Res. 328*, 235–239.
28. Clausen, M. H., Jorgensen, M. R., Thorsen, J., and Madsen, R. (2001) A strategy for chemical synthesis of selectively methylesterified oligomers of galacturonic acid. *J. Chem. Soc., Perkin Trans. 1*, 543–551.
29. Clausen, M., and Madsen, R. (2004) Synthesis of oligogalacturonates conjugated to BSA. *Carbohydr. Res. 339*, 2159–2169.
30. Clausen, M. H., and Madsen, R. (2003) Synthesis of hexasaccharide fragments of pectin. *Chem.—Eur. J. 9*, 3821–3832.
31. Petersen, B. O., Meier, S., Duus, J. O., and Clausen, M. H. (2008) Structural characterization of homogalacturonan by NMR spectroscopy-assignment of reference compounds. *Carbohydr. Res. 343*, 2830–2833.
32. Herron, S. R., Scavetta, R. D., Garrett, M., Legner, M., and Jurank, F. (2003) Characterization and implications of Ca^{2+} binding to pectate lyase C. *J. Biol. Chem. 278*, 12271–12277.
33. Morris, E. R., Powell, D. A., Gidley, M. J., and Rees, D. A. (1982) Conformations and interactions of pectins 1. Polymorphism between gel and solid states of calcium polygalacturonate. *J. Mol. Biol. 155*, 507–516.
34. Powell, D. A., Morris, E. R., Gidley, M. J., and Rees, D. A. (1982) Conformations and interactions of pectins 2. Influence of residue sequence on chain association in calcium pectate gels. *J. Mol. Biol. 155*, 517–531.
35. Walkinshaw, M. D., and Arnott, S. (1981) Conformations and interactions of pectins. 1. X-ray-diffraction analyses of sodium pectate in neutral and acidified forms. *J. Mol. Biol. 153*, 1055–1073.

36. Walkinshaw, M. D., and Arnott, S. (1981) Conformations and interactions of pectins. 2. Models for junction zones in pectinic acid and calcium pectate gels. *J. Mol. Biol. 153*, 1075–1085.
37. Jarvis, M. C., and Apperley, D. C. (1995) Chain conformation in concentrated pectic gels: Evidence from C-13 NMR. *Carbohydr. Res. 275*, 131–145.
38. Hricovini, M., Bystricky, S., and Malovikova, A. (1991) Conformations of (1−4)-linked α-D-galacturono-di-saccharides and α-D-galacturono-tri-saccharides in solution analyzed by NMR measurements and theoretical calculations. *Carbohydr. Res. 220*, 23–31.
39. Gouvion, C., Mazeau, K., Heyraud, A., Taravel, F. R., and Tvaroska, I. (1994) Conformational study of digalacturonic acid and sodium digalacturonate in solution. *Carbohydr. Res. 261*, 187–202.
40. Dinola, A., Fabrizi, G., Lamba, D., and Segre, A. L. (1994) Solution conformation of a pectic acid fragment by ^{1}H-NMR and molecular dynamics. *Biopolymers 34*, 457–462.
41. Gerlt, J. A., and Gassman, P. G. (1992) Understanding enzyme-catalyzed proton abstraction from carbon acids: Details of stepwise mechanisms for β-elimination reactions. *J. Am. Chem. Soc. 114*, 5928–5934.
42. Gerlt, J. A., and Gassman, P. G. (1993) Understanding the rates of certain enzyme-catalyzed reactions: Proton abstraction from carbon acids, acyl-transfer reactions, and displacement reactions of phosphodiesters. *J. Am. Chem. Soc. 115*, 11552–11568.
43. Jenkins, J., Shevchik, V. E., Hugouvieux-Cotte-Pattat, N., and Pickersgill, R. W. (2004) The crystal structure of pectate lyase Pel9A from *Erwinia chrysanthemi*. *J. Biol. Chem. 279*, 9139–9145.
44. Atkins, E. D. T., Nieduszy.Ia, Parker, K. D., and Smolko, E. E. (1973) Structural components of alginic acid. 2. Crystalline-structure of poly-α-L-guluronic acid: Results of X-ray-diffraction and polarized infrared studies. *Biopolymers 12*, 1879–1887.
45. Perez, S., Mazeau, K., and du Penhoat, C. H. (2000) The three-dimensional structures of the pectic polysaccharides. *Plant Physiol. Biochem. 38*, 37–55.
46. Braccini, I., Grasso, R. P., and Perez, S. (1999) Conformational and configurational features of acidic polysaccharides and their interactions with calcium ions: A molecular modeling investigation. *Carbohydr. Res. 317*, 119–130.
47. DeLano, W. L., Ed. (2002) The PyMOL molecular graphics system. 0.80 version. The PyMOL User's Manual, DeLano Scientific, San Carlos, CA
48. Wallace, A. C., Laskowski, R. A., and Thornton, J. M. (1995) LIGPLOT: A program to generate schematic diagrams of protein ligand interactions. *Protein Eng. 8*, 127–134.